LANGMUIR Article
Cite This: Langmuir 2017, 33, 14586−14591
pubs.acs.org/Langmuir

Hydrogen Uptake on Coordinatively Unsaturated Metal Sites in VSB-5: Strong Binding Affinity Leading to High-Temperature D_2/H_2 Selectivity

Amit Sharma,[†,‡] Keith V. Lawler,[*,†,§] Jarod J. Wolffis,[†] Christopher T. Eckdahl,[∥] Cooper S. McDonald,[∥] Jesse L. C. Rowsell,[⊥,#] Stephen A. FitzGerald,[∥] and Paul M. Forster[*,†,§]

[†]Department of Chemistry and Biochemistry and [§]High Pressure Science and Engineering Center, University of Nevada Las Vegas, Las Vegas, Nevada 89154, United States

[‡]Oak Ridge National Laboratory, Spallation Neutron Source, Oak Ridge, Tennessee 37831, United States

[∥]Physics and Astronomy Department and [⊥]Chemistry and Biochemistry Department, Oberlin College, Oberlin, Ohio 44074, United States

Supporting Information

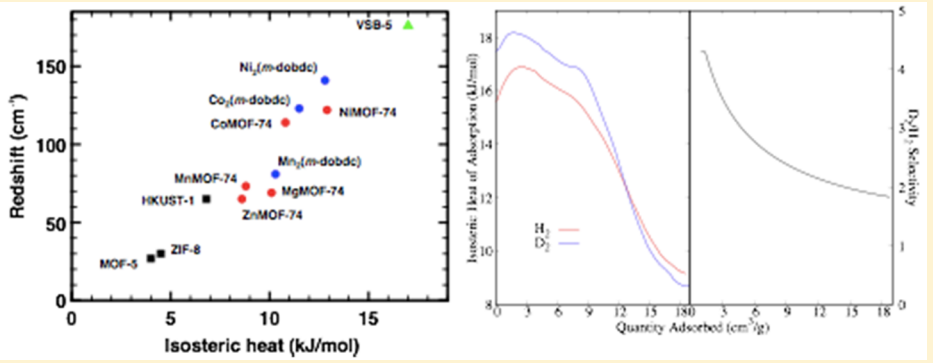

ABSTRACT: We examine the adsorption of hydrogen and deuterium into the nanoporous nickel phosphate, VSB-5. On the basis of gas sorption analysis, VSB-5 exhibits one of the highest measured H_2 heats of adsorption (HOA) for hydrogen (16 kJ/mol) yet reported. This high HOA is consistent with an unusually large red shift in the Q(1) and Q(0) hydrogen vibrational modes as measured with in situ infrared spectroscopy. The HOA for D_2 is measured to be 2 kJ/mol higher than that for H_2. "Ideal adsorbed solution theory" analysis of H_2 and D_2 isotherms provides selectivities above 4 for deuterium at 140 K, suggesting that VSB-5 is a promising adsorbent for pressure-swing adsorption-type separations of hydrogen isotopes.

INTRODUCTION

Hydrogen and its isotopes, deuterium and tritium, have numerous scientific and practical uses. In addition to its potential as an energy carrier for fuel cells, hydrogen finds extensive use in commercial chemical processes, welding, and rocket propulsion.[1−4] Many of these applications would benefit from superior storage solutions compared to high-pressure cylinders, but virtually all physisorptive storage materials investigated interact too weakly with H_2 to provide meaningful improvements.[5−7] Chemisorptive storage approaches have also been explored extensively, but the interactions are invariably stronger than ideal, leading to poor kinetics and energy efficiency.[5,8−10] An ideal interaction energy was postulated to be between 15 and 30 kJ/mol,[11−13] but very few materials have interactions in this range.

Deuterium is important commercially in drug delivery[14] and as a moderator in proliferation-resistant CANDU-type nuclear reactors. For nuclear waste processing and environmental remediation of radioactive releases, tritium-selective materials are needed. Tritium, which currently costs ca. $30 000 USD per gram, finds use in medical diagnostics, sign illumination, and military applications.[15−17] Because tritium's decay product ^{3}He has numerous critical functions such as neutron detection, improved tritium separations technologies may indirectly lead to a more stable supply of this critical isotope.[18] Scientifically, both isotopes are commonly used in neutron scattering studies, as radioactive tracers, and as low-interference solvents in nuclear magnetic resonance spectroscopy.

Current isotopic separations rely on the differences in boiling point and/or diffusivity and are nonideal due to high-energy consumption. There has been growing interest in developing adsorption-based technologies such as pressure swing adsorption (PSA) or related techniques such as temperature swing adsorption for isotope recovery as it could lead to dramatically

Received: October 13, 2017
Revised: November 16, 2017
Published: November 17, 2017

DOI: 10.1021/acs.langmuir.7b03580
Langmuir 2017, 33, 14586−14591

lower energy consumption and thus lower overall costs. PSA focuses on separation of gas molecules or adsorbates by pressurizing the gas mixture on to a sorbent to trap a certain type of molecule followed by a depressurizing step where the collected molecules are released for subsequent purification. Several properties are critical in a good PSA sorbent: it should have high selectivity for one isotope compared to that of another, and (to minimize energy consumption) it should have acceptable uptake and selectivity at relatively high temperatures, ideally room temperature.[19] A key challenge to achieving PSA-type isotopic separations is identifying materials with a usable isotopic selectivity that can function in more favorable temperature ranges. In this paper, we re-examine hydrogen uptake in a nanoporous nickel phosphate, VSB-5, demonstrating it is a very rare example of a material with a isosteric heat of adsorption (HOA) at 140 K for hydrogen in the 15−30 kJ/mol range, considered ideal for hydrogen storage applications. Further, we demonstrate that deuterium has a HOA sufficiently higher compared to hydrogen to make this material attractive for PSA-type isotopic separations.

VSB-5, $Ni_{20}[(OH)_{12}(H_2O)_6][(HPO_4)_8(PO_4)_4]\cdot 12H_2O$), was first reported by Cheetham and co-workers in 2001.[20] Exhibiting large unidimensional pores of 11 Å decorated by phosphate, hydrogen phosphate, and ligand water molecules, VSB-5 reveals a pore chemistry that is quite different from those of other crystalline nanoporous materials, leading to numerous catalytic studies.[21] At least a fraction of the ligand water molecules may be removed during activation, creating accessible, coordinatively unsaturated Ni(II) sites along the pore. In 2003, VSB-5 was evaluated for hydrogen adsorption through gas adsorption, temperature-programmed desorption, and inelastic neutron scattering measurements.[22] The authors identified a strong initial binding expected to arise from the interaction between H_2 and accessible Ni(II) sites, but a HOA was not determined.

EXPERIMENTAL SECTION

Our samples were activated for 7 days at 563 K under 10^{-6} mbar vacuum (ramp rate = 0.5 K/min). All H_2 and D_2 isotherms used for HOA determination were measured on the same sample to eliminate run-to-run variation arising from issues such as sample mass errors. We also found it necessary to carry out a brief 373 K reactivation of the sample between each measurement to ensure gas from the previous measurement diffused out of the pores and to remove trace gas which may otherwise build up in the pores over time. Adsorption isotherms were measured on a Micromeritics ASAP 2020 physisorption analyzer fitted with a He cryostat purchased from Cold-Edge technologies. The He cryostat provides ±0.01 K temperature stability and when coupled with long equilibration times helps to measure reproducible adsorption isotherms. The isotherms were collected in 10 K increments from 120 K through 140 K. Desorption isotherms were always collected to confirm negligible hysteresis.

Infrared spectra were obtained using a Bomem Da3 spectrometer with a quartz halogen source, KBr beam splitter, and mercury cadmium telluride detector. A broad-band visible filter was used to minimize sample heating by the infrared (IR) source. Measurements are performed using the diffuse reflectance technique outlined in our earlier work.[23] This technique significantly enhances the IR signal of adsorbed H_2 in comparison to traditional transmission measurements. A custom-built cryogenic chamber allows the sample powders to be mounted, degassed, cooled, and dosed with H_2 without exposing them to air.[24] Loading is performed at 77 K, after which the sample is slowly cooled to base temperature. The excess pressure drop (relative to a He reference) is used to determine the quantity of H_2 gas adsorbed. In all cases spectra are referenced to a background spectrum of the VSB-5 sample containing only He thermal exchange gas.

RESULTS AND DISCUSSION

For our reinvestigation of VSB-5, we synthesized our sample following the original recipe and phase purity was confirmed by powder X-ray diffraction. Full experimental details are provided in the Supporting Information. Gas adsorption in VSB-5 is quite sensitive to activation conditions. Thermogravimetric analysis (TGA) studies show mass loss between 470 K and 700 K with no plateau.[22] The lack of a plateau in this region suggests that the complete loss of the ligand water molecules may be incomplete before framework collapse processes (which also cause mass losses) begin. Overnight activation at 573 K resulted in a lower than expected BET surface area and gray discoloration at the edges of the sample (the activated material has a yellow color), consistent with partial framework collapse. After several measurements, we determined that the highest surface areas could be achieved by long activations at 563 K (7 days under 10^{-6} mbar vacuum). The 77 K N_2 adsorption−desorption isotherm of activated VSB-5 shows type 1 behavior with no hysteresis with a BET surface area of 420 m^2/g over the nanoporous region: $0.01 \leq P/P_0 \leq 0.08$. As the surface area is lower than the original report, the surface area was simulated using the "rolling an atom over the surface" Monte Carlo technique,[25] which predicts a 460 m^2/g surface area of ideal VSB-5 with all of the coordinated waters removed. The minor discrepancy between our measurement and the predicted ideal may result from either a small fraction of pore blockage or a minor sample mass error and should have a negligible influence on HOA determination.

Isotherms were collected at 120, 130, and 140 K to obtain reliable HOAs (Figure 1, temperature justification in the Supporting Information). All these isotherms are initially steep with a sharp inflection point in the 10−20 Torr region followed by gradual additional uptake toward the asymptotic adsorption capacity. This is consistent with the presence of strongly interacting sites (steep region) followed by additional adsorption on less strongly interacting sites. Figure 2 displays the isosteric HOA extracted via the Clausius−Clapeyron equation using the H_2 and D_2 isotherms in Figure 1. The initial HOA are around 16 kJ/mol for H_2 and 18 kJ/mol for D_2. This value drops sharply beginning around 10 cm^3/g and progressing through 15 kJ/mol, suggesting saturation of the primary sorption site and additional uptake on secondary sites. To confirm the HOA values for both H_2 and D_2, a second

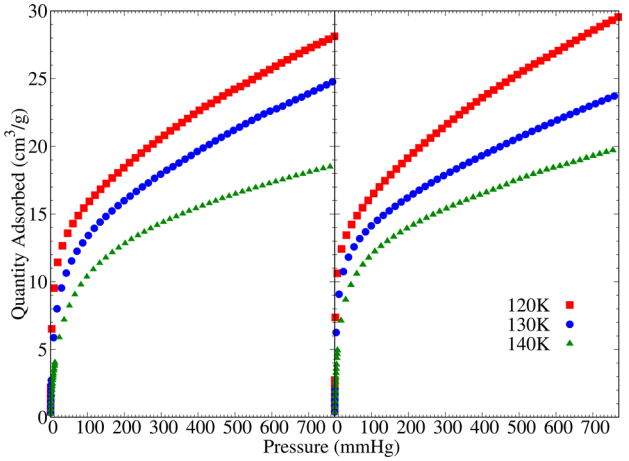

Figure 1. Measured adsorption isotherms for H_2 (left) and D_2 (right).

DOI: 10.1021/acs.langmuir.7b03580
Langmuir 2017, 33, 14586−14591

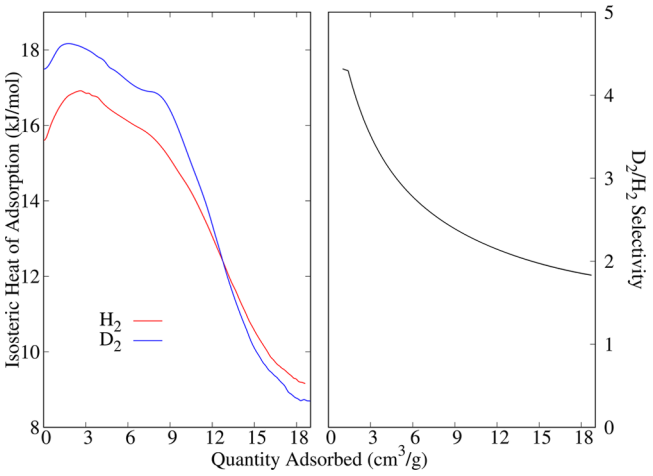

Figure 2. Measured heats of adsorption (left) and IAST determined selectivity (right) for H_2 and D_2 into VSB-5.

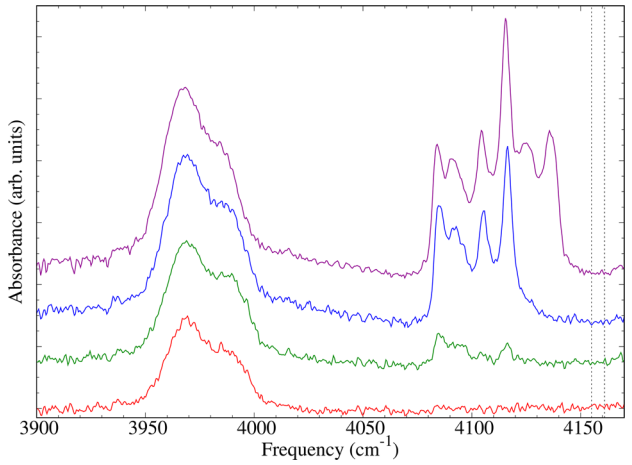

Figure 3. Diffuse reflectance IR spectra of adsorbed H_2 within VSB-5 at 40 K. Spectra are shown for H_2 concentrations in cm^3/g of: red 6 (lowest), green 17, blue 45, and purple 80 (highest).

independent study was performed at Oberlin College using a similar gas sorption analyzer with a custom-built cryostat. Initial HOA values of 16.8 and 18.4 kJ/mol obtained in that study for H_2 and D_2 respectively are within the experimental error of our values plotted above.

The 2003 study on H_2 adsorption in VSB-5 concluded that the most favorable H_2 adsorption site is a coordinatively unsaturated Ni(II) site which (presumably) becomes accessible during activation. The paper showed that a high initial slope in a H_2 gas sorption isotherm, an unusually low rotational tunneling energy measured for adsorbed H_2 with inelastic neutron scattering, and the disappearance of the steep initial slope for H_2 adsorption for samples reduced under hydrogen (presumably forming nickel hydride in place of the presumed Ni(II) site) all strongly pointed to interactions with coordinatively unsaturated metal sites as driving VSB-5's hydrogen loading. Our work is fully consistent with this interpretation, although none of our data definitively confirm this conclusion.

One puzzling feature of the HOA curve is that the site with the high affinity for hydrogen appears to saturate at loadings of approximately 12 cm^3/g. If we assume all six potential Ni(II) sites adsorb hydrogen, we would expect the high HOA region to continue up to loadings of 53 cm^3/g. Assuming Ni(II) sites are indeed responsible for the high HOA, there are several possible explanations. It is possible that only a fraction of the H_2O molecules are removed during activation. The continuous mass losses through the loss of bound waters through sample decomposition observed in TGA experiments make it impossible to quantify the precise water loss. It is also possible that a fraction of the sites are blocked by either remaining bound waters, hydrogen adsorbed to adjacent sites, or a structural rearrangement involving the (PO_4/HPO_4) groups lining the pores. We are pursuing additional data to shed light on this question which may enable us to improve activation.

Previous studies have noted a consistent red shift in the frequency of the H_2 vibrational mode relative to its gas-phase value (4161 cm^{-1}). The magnitude of the shift shows a linear correlation with the strength of the sorbent−H_2 interaction.[26,27] Although the H_2 vibration is not IR-active, interactions with the framework induce a dipole moment such that the transition can now be measured with IR spectroscopy. Figure 3 presents IR absorption spectra obtained using a customized diffuse reflectance apparatus.[24] The spectra are referenced to degassed VSB-5 and show the vibrational modes of the adsorbed H_2. At the lowest concentration only a broad absorption is observed with features at 3970 and 3986 cm^{-1}. We believe these to be the highly perturbed Q(1) and Q(0) modes, respectively. These Q(J) modes are the purely vibrational (rotational quantum number $\Delta J = 0$) excitations. Because of quantum statistics, hydrogen molecules with even J quantum numbers are constrained to have total nuclear spin $I = 0$ of the adsorbed H_2 (called para-H_2), and odd J quantum numbers have $I = 1$ (called ortho-H_2). At the temperatures studied only the $J = 0$ and $J = 1$ states are thermally populated. At higher concentrations, additional features appear in the region of 4080 to 4140 cm^{-1}. These are indicative of H_2 adsorbed at weaker secondary sites.[26] At low concentration H_2 first adsorbs in the most strongly binding (primary) site, and once this is saturated, it starts to occupy secondary sites. The primary-site H_2 modes are shifted by roughly 180 cm^{-1} relative to the corresponding gas-phase values representing the largest reported red shift for a porous material. Figure 4 shows the measured vibrational red shift as a function of HOA for a series

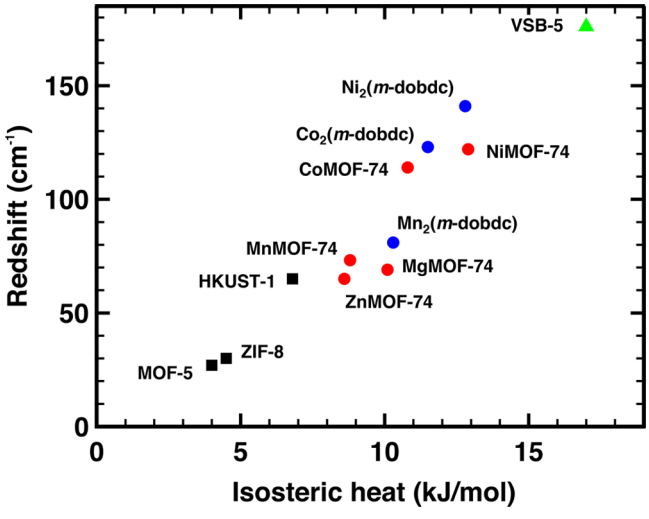

Figure 4. Measured IR red shift as a function of the initial isosteric heat of adsorption for several MOF materials.[23,26−29]

DOI: 10.1021/acs.langmuir.7b03580
Langmuir 2017, 33, 14586−14591

of MOF materials.[23,26−29] There is a strong correlation between the two, and as can be seen, our measured HOA value for VSB-5 is perfectly in line with the overall trend.

To our knowledge, VSB-5 is the second nanoporous framework demonstrated to bind hydrogen with a HOA above 15 kJ/mol. The first is a Cu(I)-based MOF with a 32 kJ/mol HOA attributed to H_2 sorption on the Cu(I) site.[30,31] While the initial H_2 adsorption in VSB-5 occurs with interactions sufficiently strong for mobile applications, VSB-5 itself is unlikely to find application for mobile hydrogen storage applications because of its modest gravimetric hydrogen uptake. The low gravimetric capacity can be rationalized from the stoichiometry; occupation of all pore-accessible Ni(II) sites leads to a maximum H_2 loading of just 0.48% hydrogen by mass. Secondary sites will raise this value to a degree, but not enough to reach United States Department of Energy targets. However, a deeper understanding of the origin of the remarkable HOA may provide useful insights to aid in the discovery of potentially useful compounds.

The initial HOA measured for D_2 in the same sample was ∼1.5 kJ/mol higher than that of H_2, a difference persisting consistently through the range presumed to arise from interaction with the metal site. At higher loadings, the HOAs converge to essentially the same value. As H_2 and D_2 are identical electronically and differ primarily by mass, this difference in HOA must come from mass-dependent quantum effects. These effects result in higher HOAs for heavier isotopes bound in the same electronic potential energy well, but with lower zero-point translational energies. Lower zero-point translational energies occur because the heavier isotope sits lower in that potential well, resulting in a stronger binding energy. Differences in HOA between H_2 and D_2 have previously been attributed to this effect for carbon nanotubes, organic frameworks, zeolites, and metal−organic frameworks.[29,31−35] In Cu(I)-MFU-4*l*,[30] the 2.5 kJ/mol HOA difference between the isotopes is attributed to this effect based on the difference in the adsorbate's vibrational frequencies: υ_r H_2 = 1427 cm^{-1}, υ_r D_2 = 1363 cm^{-1}. The difference in D_2/H_2 binding energy arising from the zero-point energies diminishes with increasing temperature, causing the measured H_2 and D_2 HOAs to converge toward identical HOAs. In single-walled carbon nanotubes, for example, the quantum effects are no longer observed by 77 K.[31] Persistence of measurable quantum effects up to at least 140 K is consistent with the exceptionally strong hydrogen binding present in VSB-5. As the quantum effects leading to the difference in HOA are primarily mass-dependent, it is reasonable to anticipate that tritium (or HT) would also exhibit a HOA difference which could be utilized for separations of this isotope.

Adsorption was simulated with grand canonical Monte Carlo using just electrostatics and a quantum (Feynman-Hibbs) corrected Lennard-Jones potential. The model was found to underpredict the experimentally observed properties, and only gives a 0.5 kJ/mol difference in the initial HOAs of D_2 and H_2 (details and plot in Supporting Information). This was also observed in HKUST-1 (which has coordinatively unsaturated metal sites),[36] where similar simulations using two different common H_2 models underpredict the measured HOA. In contrast, H_2 adsorption into MOF-5 (IRMOF-1),[37] which has no open metal sites, is well-described by those models. This failure indicates that there are more complex effects at play than those classical models describe. Recently, Space and co-workers used a polarization term to account for the missing energetics.[38] Using their model with just polarization of H_2 by the framework improved agreement between simulation and experiment, predicting a 1.2 kJ/mol difference in the initial HOAs. By applying the Feynman−Hibbs correction to the polarization term, it may be possible to further improve the quantitative prediction of the differential adsorption between H_2 and D_2 in materials with coordinatively unsaturated metal sites.

The difference in the H_2 and D_2 HOA indicate that VSB-5 will be selective for D_2. Using the slopes of the Henry's law region supplies a coarse estimate for the initial selectivity, but it is better to use ideal adsorbed solution theory (IAST).[39] IAST combines experimental isotherms of two different gases measured at the same temperature to estimate the selectivity of the material for a binary mixture of any composition across a range of loadings. The initial measured selectivity at 140 K for VSB-5 is in excess of 4 using both Henry's law slopes and IAST (IAST curve in Figure 2). We believe this is the highest measured selectivity in this temperature range, although simulations on Cu(I)−MFU-4*l* suggest a possible selectivity between 5 and 7.6 in the 120−140 K range.[30] VSB-5 surpasses NiMOF-74, which, to our knowledge, was previously the best measured high-temperature material for this separation for the same mechanistic reasons.[29] The selectivity for D_2 is highest at the initial loadings and falls smoothly for higher loadings presumably because of saturation of the coordinatively unsaturated metal sites. This implies that the selectivity, much like the difference in HOA, arises from strong quantum effects that occur when the hydrogen is confined near coordinatively unsaturated metal sites.

■ CONCLUSIONS

In conclusion, VSB-5 is shown to have one of the highest measured initial heats of adsorption, greater than 16 kJ/mol for H_2. D_2 maintained a 1.5 kJ/mol greater HOA than H_2 at low loadings. This difference leads to what we believe to be the highest measured initial D_2/H_2 selectivity in any material at a temperature above 120 K. Despite exhibiting a surface area close to the theoretically predicted maximum for all bound waters removed, the total adsorption is less than one H_2 per coordinatively unsaturated Ni(II) site, indicating that either some sites are blocked by H_2 adsorbed at neighboring sites, incomplete activations still provide surface areas near the theoretical value, or there is a structural rearrangement of VSB-5 upon activation. The high HOA and selectivity make VSB-5 an attractive sorbent for lower energy cost PSA separations of D_2/H_2 gas mixtures.

■ ASSOCIATED CONTENT

Supporting Information

The Supporting Information is available free of charge on the ACS Publications website at DOI: 10.1021/acs.langmuir.7b03580.

Powder X-ray diffraction data, temperature dependence of isothermal measurements, adsorption simulations, critical parameters and force field parameters for H_2 and D_2, simulated H_2 and D_2 adsorption isotherms and isosteric heats of adsorption, and initial heats of adsorption (PDF)

DOI: 10.1021/acs.langmuir.7b03580
Langmuir 2017, 33, 14586−14591

AUTHOR INFORMATION

Corresponding Authors

*E-mail: Paul.Forster@unlv.edu.
*E-mail: keith.lawler@unlv.edu.

ORCID

Stephen A. FitzGerald: 0000-0001-9492-9256
Paul M. Forster: 0000-0003-3319-4238

Notes

The authors declare no competing financial interest.
#Deceased.

ACKNOWLEDGMENTS

This work was supported by funding from the Department of Energy's Nuclear Energy University Program. We thank the Center for Nanophase Materials Science division at Oak Ridge National Laboratory for help in collecting powder X-ray diffraction patterns. We also thank Yongqiang Cheng (VISION beamline, ORNL) for a DFT optimized structure of VSB-5 made using computing resources available through the VirtuES project, funded by Laboratory Directed Research and Development program at ORNL.

REFERENCES

(1) Tollefson, J. Hydrogen Vehicles: Fuel of the Future? *Nature* **2010**, *464*, 1262−1264.
(2) Suban, M.; Tušek, J.; Uran, M. Use of Hydrogen in Welding Engineering in Former Times and Today. *J. Mater. Process. Technol.* **2001**, *119*, 193−198.
(3) Schlapbach, L. Technology: Hydrogen-Fuelled Vehicles. *Nature* **2009**, *460*, 809−811.
(4) Boddien, A.; Loges, B.; Junge, H.; Beller, M. Hydrogen Generation at Ambient Conditions: Application in Fuel Cells. *ChemSusChem* **2008**, *1*, 751−758.
(5) Zhao, D.; Yuan, D.; Zhou, H.-C. The Current Status of Hydrogen Storage in Metal−organic Frameworks. *Energy Environ. Sci.* **2008**, *1*, 222.
(6) Suh, M. P.; Park, H. J.; Prasad, T. K.; Lim, D.-W. Hydrogen Storage in Metal−Organic Frameworks. *Chem. Rev.* **2012**, *112*, 782−835.
(7) Rowsell, J. L. C.; Millward, A. R.; Park, K. S.; Yaghi, O. M. Hydrogen Sorption in Functionalized Metal−Organic Frameworks. *J. Am. Chem. Soc.* **2004**, *126*, 5666−5667.
(8) Zhou, L. Progress and Problems in Hydrogen Storage Methods. *Renewable Sustainable Energy Rev.* **2005**, *9*, 395−408.
(9) Zhao, Y.; Kim, Y.-H.; Dillon, A. C.; Heben, M. J.; Zhang, S. B. Hydrogen Storage in Novel Organometallic Buckyballs. *Phys. Rev. Lett.* **2005**, *94*, 155504.
(10) Schlapbach, L.; Züttel, A. Hydrogen-Storage Materials for Mobile Applications. *Nature* **2001**, *414*, 353−358.
(11) Frost, H.; Snurr, R. Q. Design Requirements for Metal-Organic Frameworks as Hydrogen Storage Materials. *J. Phys. Chem. C* **2007**, *111*, 18794−18803.
(12) Bhatia, S. K.; Myers, A. L. Optimum Conditions for Adsorptive Storage. *Langmuir* **2006**, *22*, 1688−1700.
(13) Bae, Y.-S.; Snurr, R. Q. Optimal Isosteric Heat of Adsorption for Hydrogen Storage and Delivery Using Metal−organic Frameworks. *Microporous Mesoporous Mater.* **2010**, *132*, 300−303.
(14) Lowe, D. The First Deuterated Drug Arrives http://blogs.sciencemag.org/pipeline/archives/2017/04/04/the-first-deuterated-drug-arrives (accessed Sep 17, 2017).
(15) Tam, S.-W. Porous Silicon with Embedded Tritium as a Stand-Alone Prime Power Source for Optoelectronic Applications. U.S. Patent 5605171 A, 1995.
(16) Gierszewski, P. Tritium Supply for near-Term Fusion Devices. *Fusion Eng. Des.* **1989**, *10*, 399−403.
(17) Battersby, A. R. Applications of Tritium Labeling for the Exploration of Biochemical Mechanisms. *Acc. Chem. Res.* **1972**, *5*, 148−154.
(18) Kouzes, R. T. The 3He Supply Problem. *Pacific Northwest Natl. Lab.* **2009**, 1−12.
(19) Sircar, S. Basic Research Needs for Design of Adsorptive Gas Separation Processes. *Ind. Eng. Chem. Res.* **2006**, *45*, 5435−5448.
(20) Guillou, N.; Gao, Q.; Forster, P. M.; Chang, J.-S.; Noguès, M.; Park, S.-E.; Férey, G.; Cheetham, A. K. Nickel(II) Phosphate VSB-5: A Magnetic Nanoporous Hydrogenation Catalyst with 24-Ring Tunnels. *Angew. Chem.* **2001**, *113*, 2913−2916.
(21) Timofeeva, M. N.; Panchenko, V. N.; Hasan, Z.; Jhung, S. H. Catalytic Potential of the Wonderful Chameleons: Nickel Phosphate Molecular Sieves. *Appl. Catal., A* **2013**, *455*, 71−85.
(22) Forster, P. M.; Eckert, J.; Chang, J.-S.; Park, S.-E.; Férey, G.; Cheetham, A. K. Hydrogen Adsorption in Nanoporous Nickel(II) Phosphates. *J. Am. Chem. Soc.* **2003**, *125*, 1309−1312.
(23) FitzGerald, S. A.; Allen, K.; Landerman, P.; Hopkins, J.; Matters, J.; Myers, R.; Rowsell, J. L. C. Quantum Dynamics of Adsorbed H2 in the Microporous Framework MOF-5 Analyzed Using Diffuse Reflectance Infrared Spectroscopy. *Phys. Rev. B: Condens. Matter Mater. Phys.* **2008**, *77*, 224301.
(24) FitzGerald, S. A.; Churchill, H. O. H.; Korngut, P. M.; Simmons, C. B.; Strangas, Y. E. Cryogenic Apparatus for Diffuse Reflection Infrared Spectroscopy with High-Pressure Capabilities. *Rev. Sci. Instrum.* **2006**, *77*, 093110.
(25) Düren, T.; Millange, F.; Férey, G.; Walton, K. S.; Snurr, R. Q. Calculating Geometric Surface Areas as a Characterization Tool for Metal−Organic Frameworks. *J. Phys. Chem. C* **2007**, *111*, 15350−15356.
(26) FitzGerald, S. A.; Burkholder, B.; Friedman, M.; Hopkins, J. B.; Pierce, C. J.; Schloss, J. M.; Thompson, B.; Rowsell, J. L. C. Metal-Specific Interactions of H2 Adsorbed within Isostructural Metal−Organic Frameworks. *J. Am. Chem. Soc.* **2011**, *133*, 20310−20318.
(27) Kapelewski, M. T.; Geier, S. J.; Hudson, M. R.; Stück, D.; Mason, J. A.; Nelson, J. N.; Xiao, D. J.; Hulvey, Z.; Gilmour, E.; FitzGerald, S. A.; Head-Gordon, M.; Brown, C. M.; Long, J. R. M2 (M-Dobdc) (M = Mg, Mn, Fe, Co, Ni) Metal−Organic Frameworks Exhibiting Increased Charge Density and Enhanced H2 Binding at the Open Metal Sites. *J. Am. Chem. Soc.* **2014**, *136*, 12119−12129.
(28) Zhou, W.; Wu, H.; Hartman, M. R.; Yildirim, T. Hydrogen and Methane Adsorption in Metal−Organic Frameworks: A High-Pressure Volumetric Study. *J. Phys. Chem. C* **2007**, *111*, 16131−16137.
(29) FitzGerald, S. A.; Pierce, C. J.; Rowsell, J. L. C.; Bloch, E. D.; Mason, J. A. Highly Selective Quantum Sieving of D2 from H2 by a Metal−Organic Framework As Determined by Gas Manometry and Infrared Spectroscopy. *J. Am. Chem. Soc.* **2013**, *135*, 9458−9464.
(30) Weinrauch, I.; Savchenko, I.; Denysenko, D.; Souliou, S. M.; Kim, H.-H.; Le Tacon, M.; Daemen, L. L.; Cheng, Y.; Mavrandonakis, A.; Ramirez-Cuesta, A. J.; Volkmer, D.; Schütz, G.; Hirscher, M.; Heine, T. Capture of Heavy Hydrogen Isotopes in a Metal-Organic Framework with Active Cu(I) Sites. *Nat. Commun.* **2017**, *8*, 14496.
(31) Cai, J.; Xing, Y.; Zhao, X. Quantum Sieving: Feasibility and Challenges for the Separation of Hydrogen Isotopes in Nanoporous Materials. *RSC Adv.* **2012**, *2*, 8579.
(32) Beenakker, J. J. M.; Borman, V. D.; Krylov, S. Y. Molecular Transport in Subnanometer Pores: Zero-Point Energy, Reduced Dimensionality and Quantum Sieving. *Chem. Phys. Lett.* **1995**, *232*, 379−382.
(33) Kotoh, K.; Nishikawa, T.; Kashio, Y. Multi-Component Adsorption Characteristics of Hydrogen Isotopes on Synthetic Zeolite 5a-Type at 77.4K. *J. Nucl. Sci. Technol.* **2002**, *39*, 435−441.
(34) Garberoglio, G. Quantum Sieving in Organic Frameworks. *Chem. Phys. Lett.* **2009**, *467*, 270−275.
(35) Kagita, H.; Ohba, T.; Fujimori, T.; Tanaka, H.; Hata, K.; Taira, S.; Kanoh, H.; Minami, D.; Hattori, Y.; Itoh, T.; Masu, H.; Endo, M.; Kaneko, K. Quantum Molecular Sieving Effects of H_2 and D_2 on Bundled and Nonbundled Single-Walled Carbon Nanotubes. *J. Phys. Chem. C* **2012**, *116*, 20918−20922.

DOI: 10.1021/acs.langmuir.7b03580
Langmuir 2017, 33, 14586−14591

(36) Hulvey, Z.; Lawler, K. V.; Qiao, Z.; Zhou, J.; Fairen-Jimenez, D.; Snurr, R. Q.; Ushakov, S. V.; Navrotsky, A.; Brown, C. M.; Forster, P. M. Noble Gas Adsorption in Copper Trimesate, HKUST-1: An Experimental and Computational Study. *J. Phys. Chem. C* **2013**, *117*, 20116−20126.
(37) Yang, Q.; Zhong, C. Molecular Simulation of Adsorption and Diffusion of Hydrogen in Metal−Organic Frameworks. *J. Phys. Chem. B* **2005**, *109*, 11862−11864.
(38) Pham, T.; Forrest, K. A.; Hogan, A.; McLaughlin, K.; Belof, J. L.; Eckert, J.; Space, B. Simulations of Hydrogen Sorption in Rht-MOF-1: Identifying the Binding Sites through Explicit Polarization and Quantum Rotation Calculations. *J. Mater. Chem. A* **2014**, *2*, 2088−2100.
(39) Myers, A. L.; Prausnitz, J. M. Thermodynamics of Mixed-Gas Adsorption. *AIChE J.* **1965**, *11*, 121−127.

DOI: 10.1021/acs.langmuir.7b03580
Langmuir 2017, 33, 14586−14591